IJCRT.ORG ISSN : 2320-2882

INTERNATIONAL JOURNAL OF CREATIVE RESEARCH THOUGHTS (IJCRT)

An International Open Access, Peer-reviewed, Refereed Journal

Enhancing the structural properties of Mg doped $FeAl_2O_4$ for Renewable Energy Applications: A First-Principles Approach

Harsha Verma[1,2], Manwendra K. Tripathi[1*] and Mohan L. Verma[3]

[1]Department of Metallurgical and Materials Engineering, National Institute of Technology Raipur, Raipur (Chhattisgarh) India

[2]Department of Metallurgy Engineering, Shri Rawatpura Sarkar University, Raipur

[3]Department of Applied Physics, FET-SSGI,

Shri Shankaracharya Technical Campus, Junwani, Bhilai (Chhattisgarh) India

Abstract

We have employed first-principles density functional theory (DFT) calculations to systematically explore the influence of partial substitution of Fe with Mg in $FeAl_2O_4$ on its structural properties. This strategic substitution of Mg emerges as a crucial factor in enhancing the multifunctional characteristics of the material, particularly for advanced thermocatalytic applications. Despite its promising potential, the effect of Mg incorporation on $FeAl_2O_4$ has remained unexplored from a first-principles perspective, especially in the context of solar thermochemical fuel generation and photovoltaic technologies. Our electronic density of states (DOS) analysis reveals a significant band gap upon Mg doping, when applied GGA there is no band gap and when we apply GGA+U there is band gap with 2.0 eV. Which in turn strongly modulates the electronic structure of the material making it a more efficient candidate for energy harvesting and conversion applications.

Keywords: Density Functional Theory, Electronic property, GGA+U

1. Introduction

Energy security and climate change are intrinsically linked to the continued dependence on fossil fuels, which has prompted an urgent and concerted global effort to mitigate carbon emissions through CO_2 capture, sequestration[1–3], and its subsequent transformation into valuable liquid hydrocarbon fuels[4–8]. Among the various emerging strategies, two-step solar thermochemical cycles utilizing non-volatile metal oxide redox reactions have garnered significant attention as a cmpelling alternative to conventional methods such as biomass conversion, artificial photosynthesis, and photovoltaic-driven electrolysis.

These thermochemical cycles offer distinct advantages: they operate at higher thermal efficiencies, minimize system complexity, and require fewer auxiliary components, thus reducing technological barriers and enhancing scalability. Moreover, by harnessing concentrated solar energy, these systems enable a more direct and efficient pathway for solar-to-fuel conversion, paving the way for a cleaner, more resilient, and sustainable energy future[6,9].

In recent years, Density Functional Theory (DFT) has become an essential tool for understanding and predicting materials behaviour. DFT allows researchers to study materials at the electronic/atomic level, enabling them to calculate important materials properties including structural, electronic, thermal and optical behaviour[10–13]. This makes DFT a powerful tool for designing materials tailored for specific applications[14]. Using computer simulations, researchers can predict the effect of doping in the materials, such as partially replacing Fe by Mg in $FeAl_2O_4$, leading to $Fe_{0.5}Mg_{0.5}Al_2O_4$.

Hercynite ($FeAl_2O_4$) is a member of the spinel mineral group and exhibits a solid solution with the general formula $FeAl_2O_4$. Structurally, it accommodates iron in both ferrous (Fe^{2+}) and ferric (Fe^{3+}) oxidation states, which can occupy either tetrahedral or octahedral coordination sites[15–17] within the lattice framework. As a representative of the normal spinel structure, hercynite typically exhibits a preferential cation distribution in which divalent cations (Fe^{2+}) occupy tetrahedral sites, while trivalent cations (Al^{3+} and/or Fe^{3+}) are situated in octahedral[16] coordination. This arrangement closely parallels the cation ordering observed in the classical spinel $MgAl_2O_4$, where Mg^{2+} and Al^{3+} are similarly distributed[18–20].

However, under elevated thermal conditions, the ideal cation ordering of the spinel lattice undergoes a progressive breakdown. The increased thermal energy facilitates cation migration, resulting in a redistribution of metal ions across the lattice sites. Specifically, divalent cations tend to migrate from tetrahedral to octahedral positions, while trivalent cations become increasingly disordered, occupying both tetrahedral and octahedral sites. This thermally induced cation rearrangement drives the transition from a normal to an inverse spinel configuration, significantly influencing the structural, electronic, and thermochemical behavior of the material[21].

Mg-substituted hercynite emerges as a highly promising material for high-temperature applications, including refractory materials and hydrogen production[22]. However, the Mg-substitution in hercynite has not been studied for the application of renewable energy production and photovoltaic application through first-principles approach[23].

We have investigated the effect of substitution of Fe by Mg, on $FeAl_2O_4$ through first-principles study, and explore the structural properties of $Fe_{0.5}Mg_{0.5}Al_2O_4$ which has potential application for renewable energy production and photovoltaic application with GGA and GGA+U functional.

2. Computational Methodology

The first principle calculations has been performed[24–27] using the SIESTA (Spanish Initiative for Electronic Simulations with Thousands of Atoms)[25] package. Fermi-Dirac smearing technique and 50 meV electronic temperature was used. The crystallographic information files of $FeAl_2O_4$ was obtained from Materials Project[28], having Fd3m (227) space group structure. The Perdew Burke Ernzerhof (PBE) scheme of Generalized Gradient Approximation (GGA)[29] was used as the exchange-correlation functional. GGA has been applied for structural optimization and electronic property calculation of the Section 3.1 only. The GGA calculation was done to compare our data with the literature. Since the band structure of $FeAl_2O_4$ shows no band gap while applying GGA; and GGA method is known to yield smaller band gap[30] than the actual band gap, GGA+U approach has been adopted for all other calculations.

The energy was minimized using the conventional conjugate-gradient (CG) technique until each atom's forces were less than 0.001 eV/Å. The self-consistent cycle has been performed until the energy convergence reached a value of 0.0001 Ry. The elastic constants have been computed using stress-strain method.

GGA+U[31], an extension of DFT[32,33], has also been used, which corrects the delocalization error[67] of Fe's d electrons in the GGA and the Coulomb interaction between electrons in the transition metal ions[34]. The value of U varies between 2 to 6 eV[35] in Fe-based compound. In this work, the value of U is chosen as 5.4 eV.

3. Results and Discussion

This image Figure-1 appears to represent a crystal structure model of Mg-doped $FeAl_2O_4$ (hercynite), likely visualized using a computational tool like Molden. Here's a breakdown of the elements and structure shown in the Figure-1:

Structural Description:

Atoms & Colours

- Fe (Iron): Yellow sphere, bonded to six oxygen atoms forming an FeO_6 octahedron.
- Mg (Magnesium): Brown sphere, also bonded to six oxygen atoms, forming a MgO_6 octahedron.
- Al (Aluminium): Purple spheres, forming a tetrahedral network (AlO_4) in the spinel lattice.
- O (Oxygen): Red spheres, connecting cations (Fe, Mg, Al) through shared corners.

Fe and Mg are shown in octahedral coordination, surrounded by six oxygen atoms. Al atoms form a tetrahedral cluster, a key feature of the spinel structure. This distribution reflects the spinel-type lattice, where: Divalent cations (like Mg^{2+}) can occupy either tetrahedral or octahedral sites, Trivalent cations (like Al^{3+} and Fe^{3+}) mostly occupy octahedral sites. The box enclosing the structure represents a unit cell,

the smallest repeating unit of the crystal lattice. Lattice directions a, b, and c are labeled at the corners, defining the crystallographic orientation.

This model highlights Mg substitution into the $FeAl_2O_4$ lattice, where Mg replaces Fe at specific sites, likely to investigate: Cation site preference (tetrahedral vs. octahedral), Structural distortion due to doping, Impact on electronic properties of the spinel. Such visualizations are crucial in density functional theory (DFT) studies to understand the local atomic environment, bonding geometry, and charge distribution upon doping or defect introduction.

Figure 2 shows the electronic property of Mg-doped $FeAl_2O_4$ (hercynite), The electronic structure of Mg-doped hercynite ($Fe_{0.5}Mg_{0.5}Al_2O_4$) has been investigated through density of states (DOS) analysis using both the Generalized Gradient Approximation (GGA) and GGA+U methods. In the leftmost panel, the total DOS obtained using GGA reveals a considerable density of states near the Fermi level (E_f), suggesting a metallic or small band gap behavior. However, standard GGA functionals often fail to capture the strong correlation

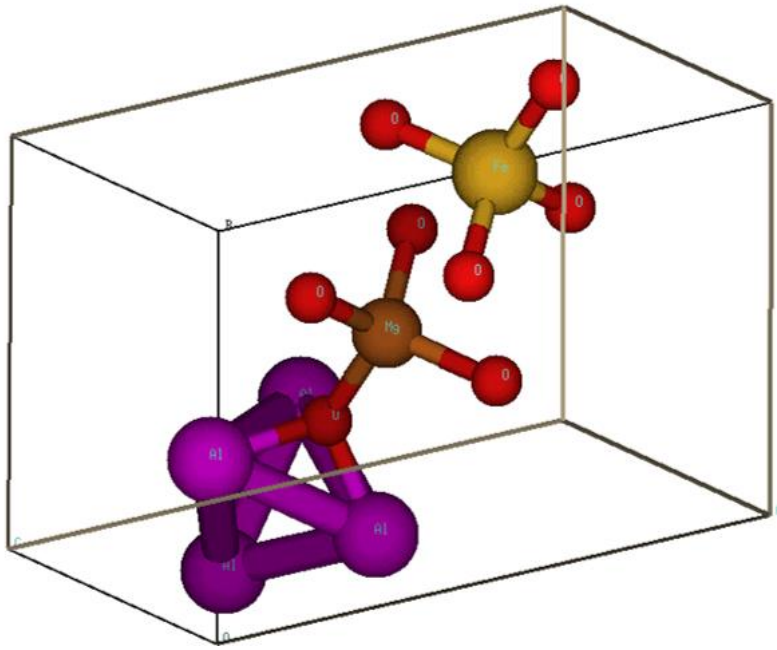

Figure 1 optimized crystal structure of $FeMgAl_2O_4$

effects associated with transition metal d-electrons, particularly those of Fe in the spinel framework.

To address this limitation, the GGA+U[35] method has been employed, as shown in the middle and right panels. The inclusion of the Hubbard U correction on Fe-3d orbitals leads to a significant modification in the electronic structure, typically resulting in the opening of a band gap or shifting of d-states, thereby indicating a transition from metallic to semiconducting nature. The projected DOS (PDOS) further highlights the orbital contributions of various atoms, where the O-2p states dominate the valence band and the Fe-3d states contribute significantly around the conduction band edge. The hybridization between Fe-3d and O-2p states suggests strong covalent interactions in the lattice. These insights are crucial for

understanding the electronic behaviour and potential redox performance of Mg-doped $FeAl_2O_4$ in solar thermochemical and catalytic applications.

The Hubbard U model provides the coulomb-energetics of two electrons, at the same site. The GGA+U[36] method usually results in an increase in the band gap compared to the GGA calculations. The U correction increases the localization of the Fe 3d electrons, which reduces the band overlap and increases the energy separation between the valence and conduction bands. GGA+U correction to $Fe_{0.5}Mg_{0.5}Al_2O_4$ leads to a more accurate and larger band gap compared to the GGA calculations, providing a better match with reported value and a more reliable description of its electronic and thermal properties[37]. It is observed that the value of U for iron-based compounds varies from 2 to 6 eV[31,38]. Here, the value of U is taken 5.4 eV for this work. The obtained band gap of 2.00 eV, as shown in Figure (2), which is in good agreement with the literature reported data (2.2eV)[37,38].

The inclusion of the Hubbard U correction on Fe-3d orbitals leads to a significant modification in the electronic structure, typically resulting in the opening of a band gap or shifting of d-states, thereby indicating a transition from metallic to semiconducting nature, which is useful for renewable hydrogen production and photovoltaic applications.

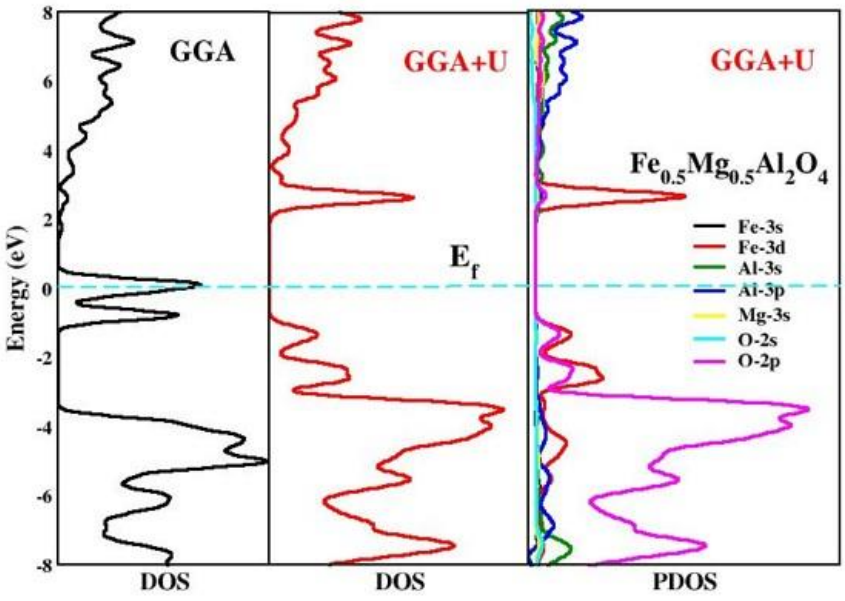

Figure 2 Electronic property of Mg doped $FeAl_2O_4$, GGA and GGA+U

4. Conclusion

Within the framework of density functional theory (DFT), first-principles calculations were carried out using the SIESTA method to investigate the structural and electronic properties of Mg doped $FeAl_2O_4$. From the electronic structure calculations, the band gap of Mg doped $FeAl_2O_4$ was determined to be 2.00 eV upon applying the GGA+U correction, which appropriately accounts for the strong correlation effects in Fe-3d orbitals. This band gap value highlights the material's semiconducting nature and its potential

suitability for applications in high-temperature solar thermochemical processes and electronic devices. Further investigation into defect-induced electronic states and their influence on charge transport can provide deeper insights into the material's functional behaviour under operating conditions.

CRediT authorship contribution statement

Harsha Verma: Conceptualization, Methodology, Visualization, Software, Writing–original draft.
Dr. Manwendra K. Tripathi: Conceptualization, Supervision, Writing–review & editing.
Dr. Mohan L. Verma: Supervision, Writing–review & editing.

Declaration of competing interest

The authors declare that they have no known competing financial interests or personal relationships that could have appeared to influence the work reported in this paper.

Data availability

Data will be made available on request.

Acknowledgments

Authors gratefully acknowledge the kind support of the Department of Metallurgical and Materials Engineering, NIT, Raipur and the management of Shri Shankaracharya Technical Campus-SSGI, Bhilai to avail computing facility in the research laboratories.

References

1. Haszeldine, R. S. Carbon Capture and Storage: How Green Can Black Be? Science **325**, 1647–1652 (2009).
2. Lackner, K. S. A Guide to CO_2 Sequestration. Science **300**, 1677–1678 (2003).
3. Elliott, S. et al. Compensation of atmospheric CO_2 buildup through engineered chemical sinkage. Geophys. Res. Lett. **28**, 1235–1238 (2001).
4. Miller, J. E. et al. Metal oxide composites and structures for ultra-high temperature solar thermochemical cycles. J. Mater. Sci. **43**, 4714–4728 (2008).
5. Olah, G. A., Prakash, G. K. S. & Goeppert, A. Anthropogenic Chemical Carbon Cycle for a Sustainable Future. J. Am. Chem. Soc. **133**, 12881–12898 (2011).
6. Chueh, W. C. et al. High-flux solar-driven thermochemical dissociation of CO2 and H2O using nonstoichiometric ceria. Science **330**, 1797–1801 (2010).
7. Chueh, W. C. & Haile, S. M. Ceria as a Thermochemical Reaction Medium for Selectively Generating Syngas or Methane from H_2 O and CO_2. ChemSusChem **2**, 735–739 (2009).

8. Rosen, B. A. et al. Ionic Liquid–Mediated Selective Conversion of CO_2 to CO at Low Overpotentials. Science **334**, 643–644 (2011).
9. Blankenship, R. E. et al. Comparing Photosynthetic and Photovoltaic Efficiencies and Recognizing the Potential for Improvement. Science **332**, 805–809 (2011).
10. Melo Quintero, J. J., Rodríguez Torres, C. E. & Errico, L. A. Ab initio calculation of structural, electronic and magnetic properties and hyperfine parameters at the Fe sites of pristine ZnFe2O4. J. Alloys Compd. **741**, 746–755 (2018).
11. Jin, C., Li, P., Mi, W. & Bai, H. Structure, magnetic, and transport properties of epitaxial ZnFe2O4 films: An experimental and first-principles study. J. Appl. Phys. **115**, 213908 (2014).
12. Řezníček, R. et al. Understanding the Mössbauer spectrum of magnetite below the Verwey transition: Ab initio calculations, simulation, and experiment. Phys. Rev. B **96**, 195124 (2017).
13. Rodríguez, K. L. S., Quintero, J. J. M., Rodríguez Torres, C. E. & Errico, L. Structural, electronic, magnetic and hyperfine properties of Fe2AlO4 and FeAl2O4. A DFT study. J. Alloys Compd. **958**, 170385 (2023).
14. Shevlin, S., Castro, B. & Li, X. Computational materials design. Nat. Mater. **20**, 727–727 (2021).
15. Jastrzębska, I. et al. Crystal structure and Mössbauer study of $FeAl_2$ O_4. Nukleonika **60**, 47–49 (2015).
16. Jastrzębska, I., Szczerba, J., Błachowski, A. & Stoch, P. Structure and microstructure evolution of hercynite spinel (Fe2+ Al2 O4) after annealing treatment. Eur. J. Mineral. **29**, 62–71 (2017).
17. Burdett, J. K., Price, G. D. & Price, S. L. Role of the crystal-field theory in determining the structures of spinels. J. Am. Chem. Soc. **104**, 92–95 (1982).
18. Dewitt, D. M., Shachar, M. H., Kodera, Y. & Garay, J. E. From nanoporous to transparent MgAl2O4 spinel—Nanostructural flexibility by reaction densification of metastable powders. Mater. Des. **211**, 110147 (2021).
19. Mohan, S. K. & Sarkar, R. Effect of in situ generated nascent magnesia and alumina from nitrate precursor on reaction sintered magnesium aluminate spinel. Mater. Des. **110**, 145–156 (2016).
20. Shi, Z., Zhao, Q., Guo, B., Ji, T. & Wang, H. A review on processing polycrystalline magnesium aluminate spinel (MgAl2O4): Sintering techniques, material properties and machinability. Mater. Des. **193**, 108858 (2020).
21. Gray, T. J. Oxide Spinels. in Refractory Materials vol. 5 77–107 (Elsevier, 1971).
22. Jastrzębska, I., Stępień, J. & Żukrowski, J. Stabilization of hercynite structure at elevated temperatures by Mg substitution. Mater. Des. **235**, 112449 (2023).

23. Takalkar, G., Bhosale, R. R., AlMomani, F., Rashid, S. & Shakoor, R. A. Ni incorporation in MgFe2O4 for improved CO2-splitting activity during solar fuel production. J. Mater. Sci. **55**, 11086–11094 (2020).
24. Kohn, W. & Sham, L. J. Self-Consistent Equations Including Exchange and Correlation Effects. Phys. Rev. **140**, A1133–A1138 (1965).
25. Soler, J. M. et al. The SIESTA method for ab initio order-N materials simulation. J. Phys. Condens. Matter **14**, 2745–2779 (2002).
26. Blaha, P., Schwarz, K., Sorantin, P. & Trickey, S. B. Full-potential, linearized augmented plane wave programs for crystalline systems. Comput. Phys. Commun. **59**, 399–415 (1990).
27. Hohenberg, P. & Kohn, W. Inhomogeneous Electron Gas. Phys. Rev. **136**, B864–B871 (1964).
28. Jain, A. et al. Commentary: The Materials Project: A materials genome approach to accelerating materials innovation. APL Mater. **1**, 011002 (2013).
29. Perdew, J. P., Burke, K. & Ernzerhof, M. Generalized Gradient Approximation Made Simple. Phys. Rev. Lett. **77**, 3865–3868 (1996).
30. Millican, S. L., Clary, J. M., Musgrave, C. B. & Lany, S. Redox Defect Thermochemistry of FeAl2O4 Hercynite in Water Splitting from First-Principles Methods. Chem. Mater. **34**, 519–528 (2022).
31. Dudarev, S. L., Botton, G. A., Savrasov, S. Y., Humphreys, C. J. & Sutton, A. P. Electron-energy-loss spectra and the structural stability of nickel oxide: An LSDA+U study. Phys. Rev. B **57**, 1505–1509 (1998).
32. Fritsch, D. & Ederer, C. Strain effects in spinel ferrite thin films from first principles calculations. J. Phys. Conf. Ser. **292**, 012014 (2011).
33. Dixit, H. et al. First-principles study of possible shallow donors in ZnAl2O4 spinel. Phys. Rev. B **87**, 174101 (2013).
34. Zhou, F., Cococcioni, M., Marianetti, C. A., Morgan, D. & Ceder, G. First-principles prediction of redox potentials in transition-metal compounds with LDA + U. Phys. Rev. B - Condens. Matter Mater. Phys. **70**, 1–8 (2004).
35. Jeng, H.-T., Guo, G. Y. & Huang, D. J. Charge-orbital ordering in low-temperature structures of magnetite: GGA+U investigations. Phys. Rev. B **74**, 195115 (2006).
36. Tolba, S. A., Gameel, K. M., Ali, B. A., Almossalami, H. A. & Allam, N. K. The DFT+U: Approaches, Accuracy, and Applications. in Density Functional Calculations - Recent Progresses of Theory and Application (ed. Yang, G.) (InTech, 2018). doi:10.5772/intechopen.72020.

37. Trottier, R. M., Bare, Z. J. L., Millican, S. L. & Musgrave, C. B. Predicting Spinel Disorder and Its Effect on Oxygen Transport Kinetics in Hercynite. ACS Appl. Mater. Interfaces **12**, 23831–23843 (2020).

38. Khalid, M., Riaz, S., Azam, M. & Naseem, S. Theoretical study of spinel structure of FeAl2O4 using density functional theory. Adv. Civ. Enviromental Mater. Res. 24–28 (2014).